Electron. Mater. Lett., Vol. 11, No. 5 (2015), pp. 828-835
DOI: 10.1007/s13391-015-4495-1

Large Electric Field-Induced Strain and Piezoelectric Responses of Lead-Free $Bi_{0.5}(Na_{0.80}K_{0.20})_{0.5}TiO_3$-$Ba(Ti_{0.90}Sn_{0.10})O_3$ Ceramics Near Morphotropic Phase Boundary

Pharatree Jaita,[1] Anucha Watcharapasorn,[1,2] Nitish Kumar,[3] David P. Cann,[3] and Sukanda Jiansirisomboon[4,*]

[1]Department of Physics and Materials Science, Faculty of Science, Chiang Mai University, Chiang Mai 50200, Thailand
[2]Materials Science Research Center, Faculty of Science, Chiang Mai University, Chiang Mai 50200, Thailand
[3]Materials Science, School of Mechanical, Industrial and Manufacturing Engineering, Oregon State University, Corvallis, OR 97331, USA
[4]School of Ceramic Engineering, Suranaree University of Technology, Nakhon Ratchasima, 30000, Thailand

(received date: 14 November 2014 / accepted date: 23 February 2015 / published date: 10 September 2015)

Lead-free piezoelectric ceramics with compositions belonging to family of compositions (1-x)$Bi_{0.5}(Na_{0.80}K_{0.20})_{0.5}TiO_3$-$xBa(Ti_{0.90}Sn_{0.10})O_3$ or (1-x) BNKT-xBTS (when x = 0.05 - 0.15 mol fraction) near the morphotropic phase boundary (MPB) were fabricated by a conventional mixed oxide method. Sintered samples had relative densities greater than 98% of their theoretical values. X-ray diffraction data revealed that the MPB region consisted of coexisting rhombohedral and tetragonal phases in the BNKT-BTS system was identified over the entire compositional range. A large electric field-induced strain (S_{max}) of 0.36% and a normalized strain coefficient (d^*_{33}) of 649 pm/V were observed in the BNKT-0.05BTS sample. The sample close to the MPB composition (BNKT-0.11BTS) exhibited the maximum dielectric constant (ε_r = 1770), temperature of maximum permittivity (T_m = 333C°) and low-field piezoelectric coefficient (d_{33} = 227 pC/N), along with reasonable ferroelectric properties (P_r = 20.6 mC/cm^2, R_{sq} = 0.88) and strain properties (d^*_{33} = 445 pm/V and S_{max} = 0.24%).

Keywords: electric field-induced strain, piezoelectric, dielectric, ferroelectric, lead free

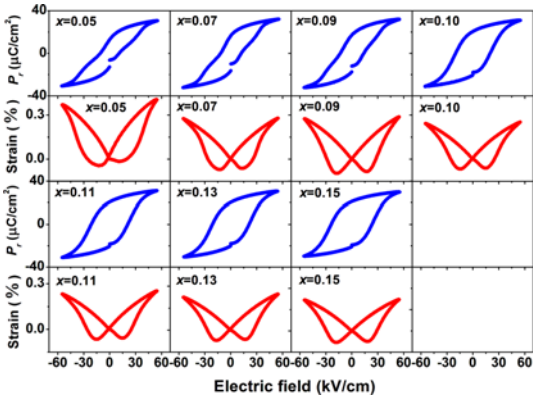

1. INTRODUCTION

PZT-based ceramics have been the dominant piezoelectric material for a half century. They are widely used in various applications such as actuators, sensors and ultrasonic transducers.[1] The compositions near the morphotropic phase boundary (MPB) in PZT-based ceramics have attracted great attention because of their excellent electromechanical properties.[2] However, with the potential for regulations (RoHS/WEEE) that may restrict the use of hazardous substances in electronic devices, intensive efforts have been devoted to search for lead-free piezoelectric materials to serve as a substitute for PZT-based ceramics. In searching for high-performance lead-free piezoelectric ceramics, the MPB between two end members with different crystal structures has been one of the main strategies.

Within the MPB region, maximum polarization values are attainable which leads to enhanced electrical properties.[2] Much attention has been paid to BNT-based solid solutions[3-7]

*Corresponding author: sukanda.jian@cmu.ac.th

because of their outstanding dielectric, ferroelectric and piezoelectric properties at compositions near the MPB. Generally the MPB region of the binary system is constrained to a very narrow range. For BNT-BKT or $Bi_{0.5}(Na_{1-x}K_x)TiO_3$ system, the MPB region was found over the range of x = 0.16 - 0.20. The $Bi_{0.5}(Na_{0.80}K_{0.20})_{0.5}TiO_3$ composition near the MPB possesses excellent ferroelectric (P_r = 38 μC/cm^2) and piezoelectric properties (d_{33} = 167 pC/N, d_{31} = 46.9 pC/N, S_{max} = 0.19%, d^*_{33} = 240 pV/m and k_{33} = 0.56).[3,4] In addition, BNKT ceramics at the MPB have been modified by ionic substitution on the A and/or B-site in order to improve the dielectric and piezoelectric properties; for examples, $BiAlO_3$-modified $Bi_{0.5}(Na_{0.80}K_{0.20})_{0.5}TiO_3$,[5] $Bi_{0.5}(Na_{0.78}K_{0.22})_{0.5}TiO_3$-$(Bi_{0.5}La_{0.5})AlO_3$,[6] $Bi_{0.5}(Na_{0.84}K_{0.16})_{0.5}TiO_3$-$Ba(Zr_{0.04}Ti_{0.96})O_3$[7] and $Bi_{0.5}(Na_{0.80}K_{0.20})_{0.5}TiO_3$-$(Ba_{0.7}Sr_{0.3})TiO_3$.[8] All of these systems have demonstrated improvements in piezoelectric properties and facile poling. Our preliminary research has also indicated that $Ba(Ti_{0.90}Sn_{0.10})O_3$ was an effective additive for improving the piezoelectric properties of $Bi_{0.5}(Na_{0.80}K_{0.20})_{0.5}TiO_3$. The results showed that the BNKT-0.10BST composition exhibited an optimum low-field piezoelectric coefficient (d_{33}) of 215pC/N.[9]

However, in this work, $Ba(Ti_{0.90}Sn_{0.10})O_3$ was added to $Bi_{0.5}(Na_{0.80}K_{0.20})_{0.5}TiO_3$ ceramics to form solid solution of (1-x)$Bi_{0.5}(Na_{0.80}K_{0.20})_{0.5}TiO_3$-$xBa(Ti_{0.90}Sn_{0.10})O_3$ or (1-x)BNKT-xBTS. This work is focused on the narrow MPB region x = 0.05 - 0.15 mol fraction. Further study in detail for MPB region of this system is necessary. The insight on composition dependent electrical properties would be beneficial to confirm the composition with the maximum piezoelectric responses. A systematic investigation on the electrical properties of refined compositions within the MPB region may also be helpful for further optimizing and understanding their functional properties and ultimately highlighting the most appropriate material for piezoelectric applications.

Moreover, to the best of our knowledge, there are currently no reports on the binary system of $Bi_{0.5}(Na_{0.80}K_{0.20})_{0.5}TiO_3$-$Ba(Ti_{0.90}Sn_{0.10})O_3$ or BNKT-BTS to date. For $Ba(Ti_{0.90}Sn_{0.10})O_3$, it has been used in various applications such as capacitor, actuator and microwave phase shifter because of its high permittivity (~7500) and bias field sensitivity. It was expected that these new lead-free piezoelectric (1-x)BNKT-xBTS ceramics near the MPB composition would show superior electrical properties compared to the unmodified and previously modified BNKT ceramics.

2. EXPERIMENTAL PROCEDURE

A conventional mixed-oxide technique was used to synthesizes $Bi_{0.5}(Na_{0.80}K_{0.20})_{0.5}TiO_3$ or BNKT and $Ba(Ti_{0.90}Sn_{0.10})O_3$ or BTS powders. Regent-grade powders of Bi_2O_3 (98%, Fluka), Na_2CO_3 (99.5%, Carlo Erba), TiO_2 (99%, Riedel-de Haën), K_2CO_3 (99%, Riedel-de Haën), $BaCO_3$ (98.5%, Fluka) and SnO_2 (99.9%, Sigma-Aldrich) were used as the starting raw materials. All carbonate powders were first dried at 120°C for 24 h to remove any moisture. The raw materials of BNKT and BTS were stoichiometrically weight and mixed by ball milling in 99.9% ethanol for 24 h and the slurry was dried using an oven. Dried BNKT and BTS powders were separately calcined in a closed Al_2O_3 crucible at 900°C and 1200°C for 2 h, respectively. Both calcined powders were then weighed and mixed in order to produce an appropriate stoichiometry for the compositions (1-x) BNKT-xBTS with x = 0.05, 0.07, 0.09, 0.10, 0.11, 0.13 and 0.15 mol fraction. After drying and sieving, the powders were granulated by adding a few drops of 3 wt. % PVA as a binder and then pressed into disks with 10 mm in diameterand about 1.3 mm in thickness. The pellets were then preheated in air at 500°C for 1 h to remove organic binder and then sintered at 1125°C for 2 h dwell time with a heating/cooling rate of 5°C/min.

An x-ray diffractometer (XRD-Phillip, X-pert) was used to identify phase of powder and sintered ceramics in 2θ = 20 - 70°. Bulk densities of all ceramics was determined using the Archimedes' method. The relative density of all samples was calculated based on the theoretical densities of BNKT (5.84 g/cm^3)[10] and BT (6.01 g/cm^3).[11] The surface morphologies of the sintered ceramics was observed using a field-emission scanning electron microscope (FE-SEM, JEOL JSM-6335F). The grain size of each sample was determined by a mean linear interception method from the SEM micrographs.

For electrical measurements, all samples were polished to 1 mm thickness and high temperature silver paste was fired on both sides at 700°C for 15 min to form the electrodes. Temperature dependence of the dielectric properties was measured using a 4284A LCR-meter over a temperature range of 25 - 500°C at a frequency of 10 kHz. A ferroelectric test system based on Radiant Technology was used to measure the polarization-electric field (*P-E*) hysteresis behavior. An AC electric field of 55 kV/cm at a frequency of 1 Hz was utilized in the hysteresis measurement. Electro-mechanical strain measurements were taken with the Radiant Technology ferroelectric system in conjunction with MTI Instruments 2100 Fotonic Sensor. Again, an electric field of 55 kV/cm at a frequency of 0.1 Hz was utilized to determine the butterfly curve or bipolar strain-electric field (*S-E*) curve. The samples were poled in silicone oil at 60°C under DC electric field of 5.5 kV/mm for 15 min. The low-field piezoelectric coefficient (d_{33}) was measured after aging for at least 24 h using d_{33}-meter (KCF technologies, S5865).

3. RESULTS AND DISCUSSION

After sintering the pellet-shaped samples at 1125°C for 2 h dwell time with a heating/cooling rate of 5°C/min, it was

Table 1. Physical, microstructure and electrical properties of (1-*x*)BNKT-*x*BTS ceramics.

x	Relative density (%)	Grain size (μm)	T_d (°C)	T_m (°C)	P_r^a (μC/cm^2)	E_c^a (kV/cm)	ε_r	d_{33} (pC/N)	S_{max} (%)	S_{neg} (%)	d^*_{33} (pm/V)
0.05	99.14 ± 0.39	0.40 ± 0.04	153	321	12.80	10.90	1600	174	0.36	- 0.02	649
0.07	99.08 ± 0.11	0.40 ± 0.03	154	328	16.47	11.75	1654	185	0.28	- 0.06	505
0.09	98.93 ± 0.21	0.40 ± 0.05	155	331	17.22	13.40	1699	203	0.28	- 0.08	508
0.10	98.88 ± 0.68	0.44 ± 0.04	159	333	20.49	19.92	1721	215	0.25	- 0.07	450
0.11	98.83 ± 0.01	0.46 ± 0.08	168	333	20.60	21.05	1770	227	0.24	- 0.07	445
0.13	98.80 ± 0.01	0.56 ± 0.08	171	323	20.27	21.28	1683	178	0.23	- 0.07	440
0.15	98.77 ± 0.39	0.57 ± 0.08	178	322	20.88	23.55	1482	153	0.23	- 0.07	409

[a]Ferroelectric data obtained at room temperature (25°C) and a frequency of 1 Hz.

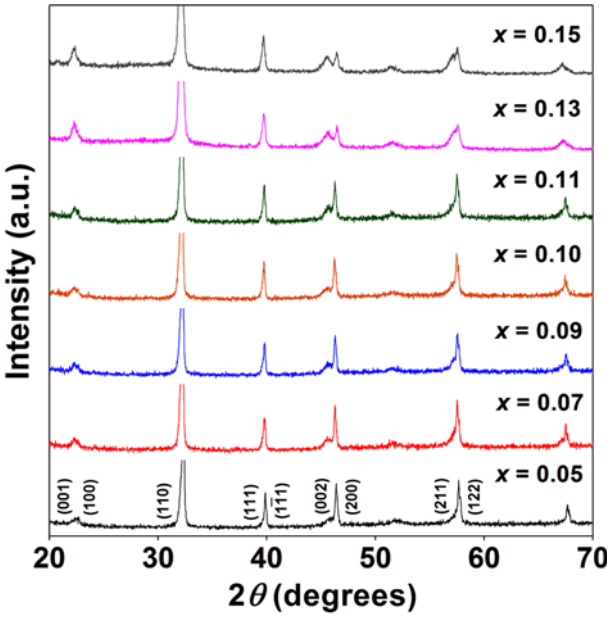

Fig. 1. X-ray diffraction patterns of (1-*x*)BNKT-*x*BTS ceramics sintered at 1125°C for 2 h with 2θ= 20 - 70°.

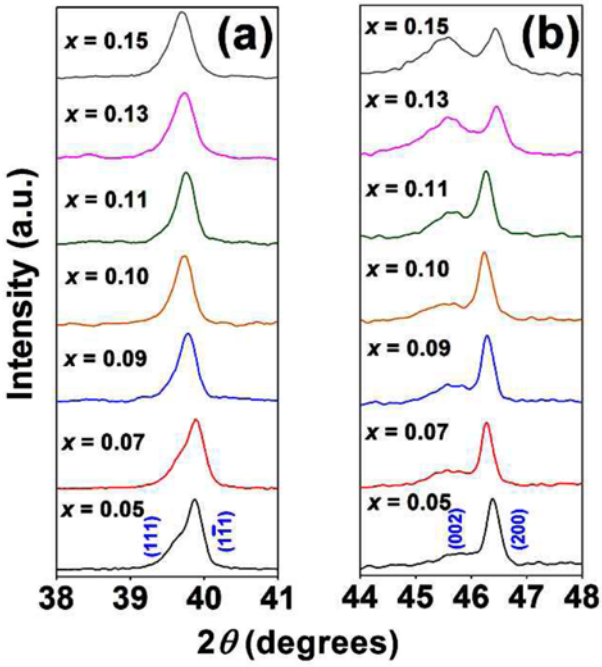

Fig. 2. X-ray diffraction patterns of (1-*x*)BNKT-*x*BTS ceramics sintered at 1125°C for 2 h where (a) 2θ= 38 - 41° and (b) 2θ= 44 - 48°.

found that high relative densities of 98 - 99% were obtained for all compositions and bulk density values exhibited a narrow range from 5.77 - 5.82 g/cm^3 (Table 1). Based on the relative density values in Table 1, the data clearly show that the addition of BTS into BNKT ceramic caused a slight decrease in samples' relative density.

X-ray diffraction data on the sintered ceramics are shown in Fig. 1. All compositions exhibited a single perovskite phase at room temperature without any secondary phases within the detection limits of XRD. A series of stable solid solutions were formed between BNKT and BTS, confirming that the starting reagents reacted completely. With increasing BTS content, the diffraction peaks shifted to lower 2θ angles indicating an increase in the unit cell size. The magnitudes of the shifts were increased proportional to the concentration of BTS in the sample. This is expected because the ionic radius of Ba^{2+} (1.42 Å) is significantly larger than that of Bi^{3+} (1.17 Å), Na^+ (1.18 Å), K^+ (1.33 Å) and the B-cation Sn^{4+} (0.81 Å) is larger than Ti^{4+} (0.74 Å).[12]

A detailed view of the XRD data in Figs. 2(a) and (b) suggests that the MPB region consists of coexisting rhombohedral and tetragonal phases over the entire compositional range. The composition BNKT-0.05BTS is likely a mixture of rhombohedral and tetragonal phases but with a higher volume fraction of rhombohedral phase over tetragonal phase. This is clearly seen by a noticeable splitting of (111)/(1$\bar{1}$1) peaks at $2\theta \sim 40°$.[13] With an increase in the BTS mole content, the splitting in the (111)/(1$\bar{1}$1) peaks decreases and the peak shape becomes nearly symmetric for compositions near x = 0.15. The compositional trend in the splitting in the

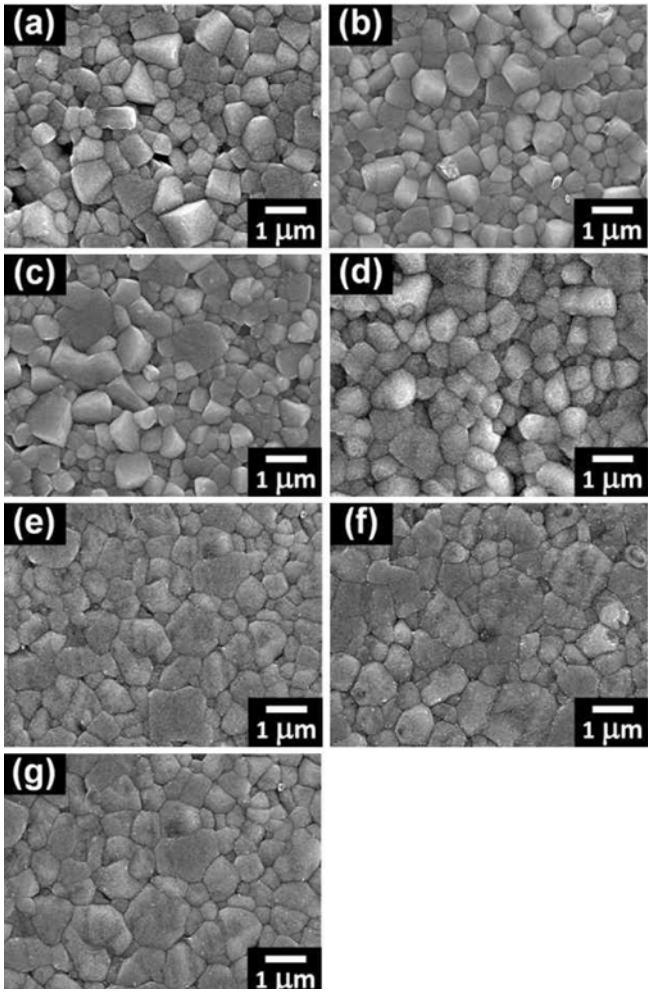

Fig. 3. Thermally etched surfaces of (1-*x*)BNKT-*x*BTS ceramics sintered at 1125°C for 2 h where (a) $x = 0.05$, (b) $x = 0.07$, (c) $x = 0.09$, (d) $x = 0.10$, (e) $x = 0.11$, (f) $x = 0.13$ and (g) $x = 0.15$.

(002)/(200) peaks is more complex. With an increase in BTS content, the splitting becomes more apparent however the peak shape is not clearly attributable to a doublet peak as expected for a single tetragonal phase. In fact, the integrated intensity of the (002) peak becomes comparable to the (002)/(200) peak. This could suggest texturing in the microstructure or the presence of multiple phases. Nonetheless, the addition of BTS would be expected to enhance the tetragonal distortions[6] and the splitting of the (002)/(200) peaks does increase as shown in Fig. 2(b).

SEM micrographs of polished and thermally etched surfaces of BNKT-BTS ceramics are shown in Fig. 3. SEM observation confirmed that all samples were considerably dense with well-developed microstructure and granular morphology which were correlated with high relative densities of 98 - 99%. The average grain size values of all compositions was found to range from 0.40 - 0.57 μm (Table 1). The addition of 5 - 11 mol. % BTS into BNKT had no

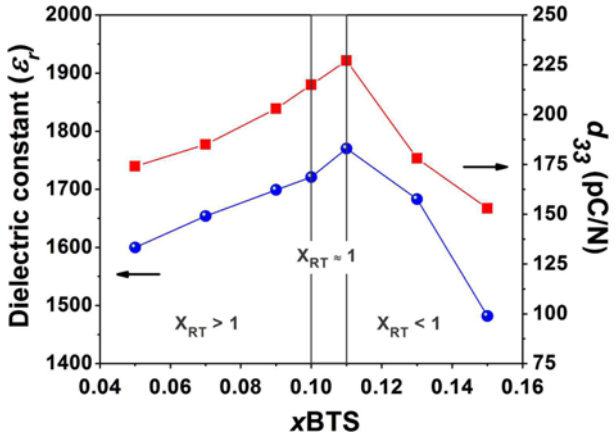

Fig. 4. Plot of room temperature dielectric constant (ε_r) and low-field piezoelectric coefficient (d_{33}) as a function of BTS content. $X_{RT} = f_{Rhombehedral}/f_{Tetragonal}$, where f = the fraction of rhombohedral and tetragonal phases.

significant influence on grain size and the values were similar (0.40 - 0.46 μm). However, average grain size values tended to slightly increase to around 0.56 - 0.57 μm with further increasing of BTS up to 13 - 15 mol. % and somewhat coarse grains formed near these compositions.

A plot of the room temperature dielectric constant (ε_r) and low-field piezoelectric coefficient (d_{33}) as a function of BTS content is shown in Fig. 4. The ε_r initially increased with increasing BTS content and reached a maximum value of 1770 for the BNKT-0.11BTS composition. It should be noted that the ε_r value for the BNKT-0.11BTS sample in this work were much higher than the value observed by Chen *et al.* ($\varepsilon_r \sim 949$) for the BNKT-0.06BZT system near the MPB composition.[7] With further increase in BTS content above $x = 0.11$, ε_r decreased to a minimum value of 1482. In addition, the piezoelectric behavior showed similar trend with increasing BTS content to that of the dielectric properties. The low-field d_{33} value increased from 174 pC/N for the BNKT-0.05BTS composition to a maximum value of 227 pC/N for the BNKT-0.11BTS composition. At higher BTS content, the d_{33} value was found to decrease to a minimum value of 153 pC/N. It can be seen that the dielectric and low-field piezoelectric properties exhibited a strong compositional and phase dependence within the MPB region of the BNKT-BTS system. While the XRD data was not conclusive in determining the coexistence of rhombohedral and tetragonal phases, this behavior suggests that an exist at approximately 11 mol. % BTS due to the enhanced dielectric and piezoelectric activity.[14] This results is consistent with the finding of Lee *et al.*[15] where the crystal structure changed from a rhombohedral-rich phase to a tetragonal-rich phase for BST content at 6 mol. % in the $(Bi_{0.5}Na_{0.5})TiO_3$-$(Ba_{0.7}Sr_{0.3})TiO_3$ system, with a similar enhancement in dielectric and piezoelectric response.

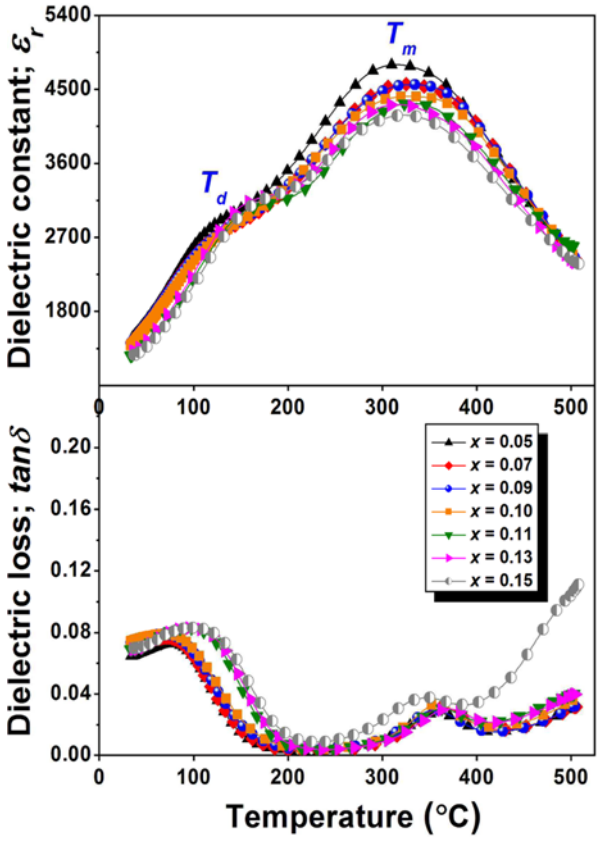

Fig. 5. Temperature dependence on dielectric constant (ε_r) and dielectric loss ($tan\delta$) of (1-x)BNKT-xBTS ceramics, measured at a frequency of 10 kHz.

Figure 5 shows temperature dependence of the dielectric constant (ε_r) and dielectric loss ($tan\delta$) for (1-x)BNKT-xBTS ceramics measured at a frequency of 10 kHz. Two dielectric anomalies, designated as T_d and T_m, were observed in the dielectric spectra of all BNKT-BTS compositions, which corroborates with the previously obtained dielectric behavior of BNT and other BNT-based ceramics.[3-7,10,14] The depolarization temperature (T_d), corresponds to the relaxor transition from an ergodic to a non-ergodic state. The temperature at which e_r reached a maximum value (T_m) corresponds to a diffuse transition. It's generally accepted that there is no phase transition across T_m in relaxors. It's a consequence of size distribution of polar nano regions, which also gives rise to frequency dependence.[16] The dielectric spectra of all BNKT-BTS ceramics exhibited broad T_d and T_m peaks which could be attributed to compositional fluctuations occurring at A and/or B-site cations and resulting in disorder and change in the perovskite unit cell.[17,18] This behavior suggested that BTS induced a diffuse phase transition in the BNKT-BTS system. Diffuse phase transitions have commonly been observed in other BNT-based ceramic systems in which either the A-site or B-site is occupied by at least two different cations.[18] Both T_d and T_m values increased with increasing BTS content. The T_m reached a maximum value of 333°C for the composition close to the MPB with x = 0.10 - 0.11. With further increasing BTS content up to 13 - 15 mol. %, a slight decrease in T_m values was observed. Chen *et al.*[7] who studied the addition $Ba(Zr_{0.04}Ti_{0.96})O_3$ into $Bi_{0.5}(Na_{0.84}K_{0.16})_{0.5}TiO_3$ ceramics also found similar an

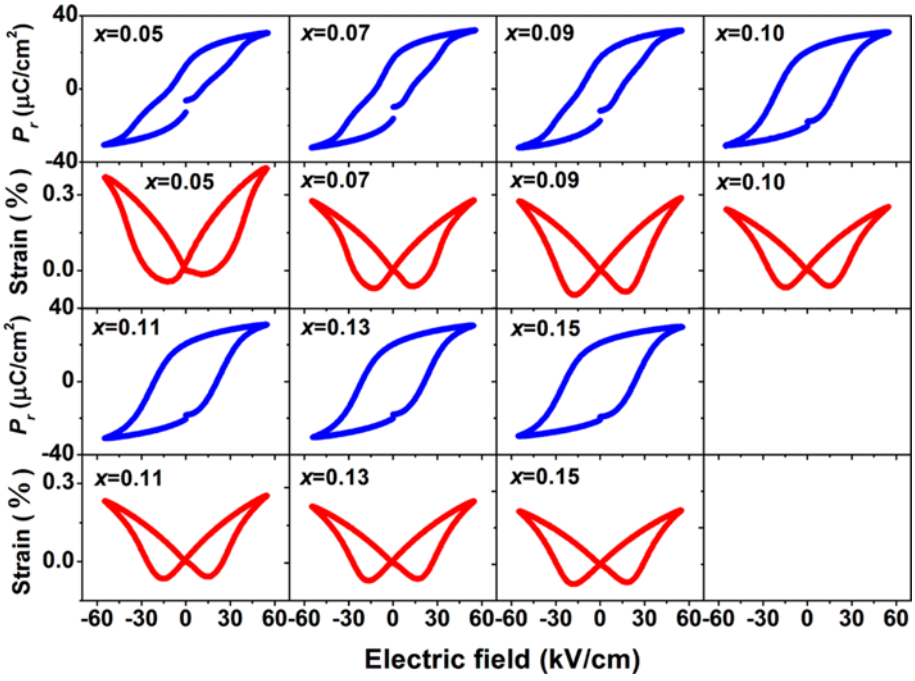

Fig. 6. Polarization-electric field (*P-E*) hysteresis loops and bipolar strain-electric field (*S-E*) of (1-x)BNKT-xBTS ceramics, measured at room temperature, under an electric field of 55 kV/cm where x = 0.05 - 0.15.

enlargement of unit cell and then decreasing T_m value. In contrast to T_m, T_d value was found to increase with BTS concentration up to maximum amount used in this study. This indicates that ionic substitution with BTS stabilized ferroelectric ordering. This is also related to the large tetragonal splitting seen in the XRD data (Fig. 2).

Figure 6 shows polarization-electric field (*P-E*) hysteresis data for (1-*x*)BNKT-*x*BTS system compositions obtained at room temperature (25°C). The P_r and E_c values determined from the data, were listed in Table 1. All samples showed well saturated *P-E* loops at room temperature. It is clear from Fig. 6 that BTS had a noticeable influence on the hysteresis behavior. Bipolar strain-electric field (*S-E*) curves of (1-*x*)BNKT-*x*BTS ceramics measured at room temperature under a maximum electric field of 55 kV/cm and a frequency of 0.1 Hz are also shown in Fig. 6. The maximum strain (S_{max}), negative strain (S_{neg}, *i.e.* the difference between zero-field strain and the lowest strain[19]), and normalized strain coefficient ($d^*_{33}= S_{max}/E_{max}$) are also listed in Table 1. A large strain of 0.36% and d^*_{33} of 649 pm/V were obtained for BNKT-0.05BTS composition. The d^*_{33} value of this BNKT-0.05BTS studied was much higher than these reported for other polycrystalline lead-free systems.[5,19,20] The emergence of such large strain was accompanied by a significant reduction in S_{neg} of −0.02%. Giant strain and behavior of bipolar *S-E* loops were similarly found in many recent works on BNT-based ceramics.[5-7,18-24] With further increasing BTS content up to 7 - 15 mol. %, the bipolar *S-E* loops exhibited back to normal butterfly-like strain loops. An increase in S_{neg} to around - 0.06 to - 0.08% was observed. This corresponded to an increase in P_r from 12.80 μC/cm^2 to around 20 - 21 μC/cm^2 with increasing E_c value (Table 1). Correspondingly, a slight decrease in S_{max} and d^*_{33} values were observed at higher concentrations of BTS. The addition of 15 mol. % BTS was found to decrease S_{max} and d^*_{33} to the minimum values of 0.23% and 409 pm/V, respectively.

All the above characteristics are typical of BNT-based ceramics. In the ceramic system studied in this work, in essence BTS was added to an MPB 80BNT-20BKT or $Bi_{0.5}(Na_{0.80}K_{0.20})_{0.5}TiO_3$ composition. As has been reported earlier, BTS is a stable ferroelectric ceramic with a Curie temperature of ~60°C.[25] As Sn replaces Ti in BTS, the Curie temperature goes down and above 20% substitution level, it starts to exhibit relaxor behavior.[25] Therefore, the BTS in this study (which has 10% Ti substituted by Sn) should be expected to have ferroelectric ordering at room temperature. Therefore, addition of more BTS to the solid solution should impart more ferroelectric characteristics to the *P-E* and *S-E* curves like similar ceramic systems *e.g.* BNT-BKT-BT and others.[4,26] As was seen earlier, this was supported by the XRD data (Fig. 1 and Fig. 2) as well where the (200) peak splitting enhanced as the amount of BTS content increased. With increase in the content of stable

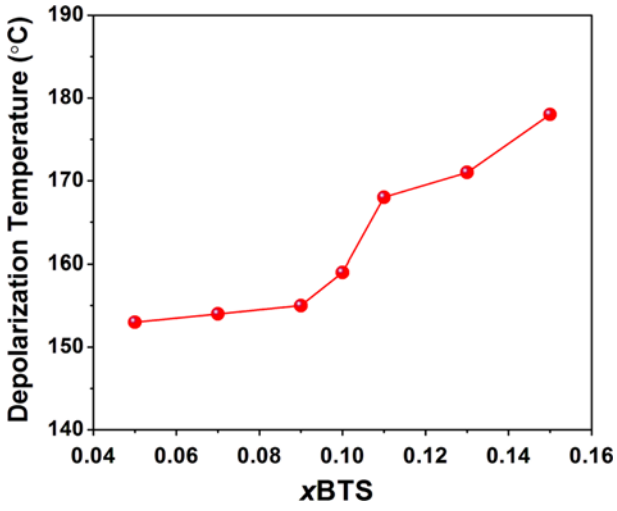

Fig. 7. Plots of depolarization temperature as a function of BTS content.

ferroelectric end-member in the solid solution, an increase in domain stability should be expected. This could be seen in Fig. 6, where the polarization curves transitioned from pinched to more ferroelectric-like behavior as the amount of BTS increased in the solid solution. A similar characteristic was observed in *S-E* curves as well where negative strain increased with BTS content. These suggested that the compositions transitioned from ergodic behavior where domains are unstable in absence of electric field, to a non-ergodic relaxor behavior where domains are stable even in absence of electric field after a relaxor to ferroelectric transformation has occurred on application of high-enough electric fields. It was reflected in the P_r and E_c values as well as listed in Table 1. A non-ergodic composition is in general expected to have higher E_c and P_r values. An increase in domain stability was also supported by increase in depolarization temperature with BTS content (Fig. 7 and Table 1), where it could be seen that T_d increased from 153°C to 178°C as BTS content increased from 5 to 15 mol. % in the solid solution. This indicated that the compositions with more BTS were more non-ergodic at room temperature and thus had higher domain stability. A decrease in d^*_{33} with BTS content could be attributed to increase in tetragonality in polycrystalline ceramics, where constraints put by grain boundaries makes it more difficult for domains to move as the tetragonal behavior increases.

Figure 8 shows the evolution of polarization loops for various compositions with temperature. It supported the argument presented above regarding the stability of domains and non-ergodic to ergodic transition as well. In general, a pinched *P-E* behavior indicates the onset of ergodic behavior. It could be seen in Fig. 8 that for 5% BTS composition, the loop was pinched at a temperature as low as 50°C. On the other hand, for 15% BTS composition, the pinched-loop

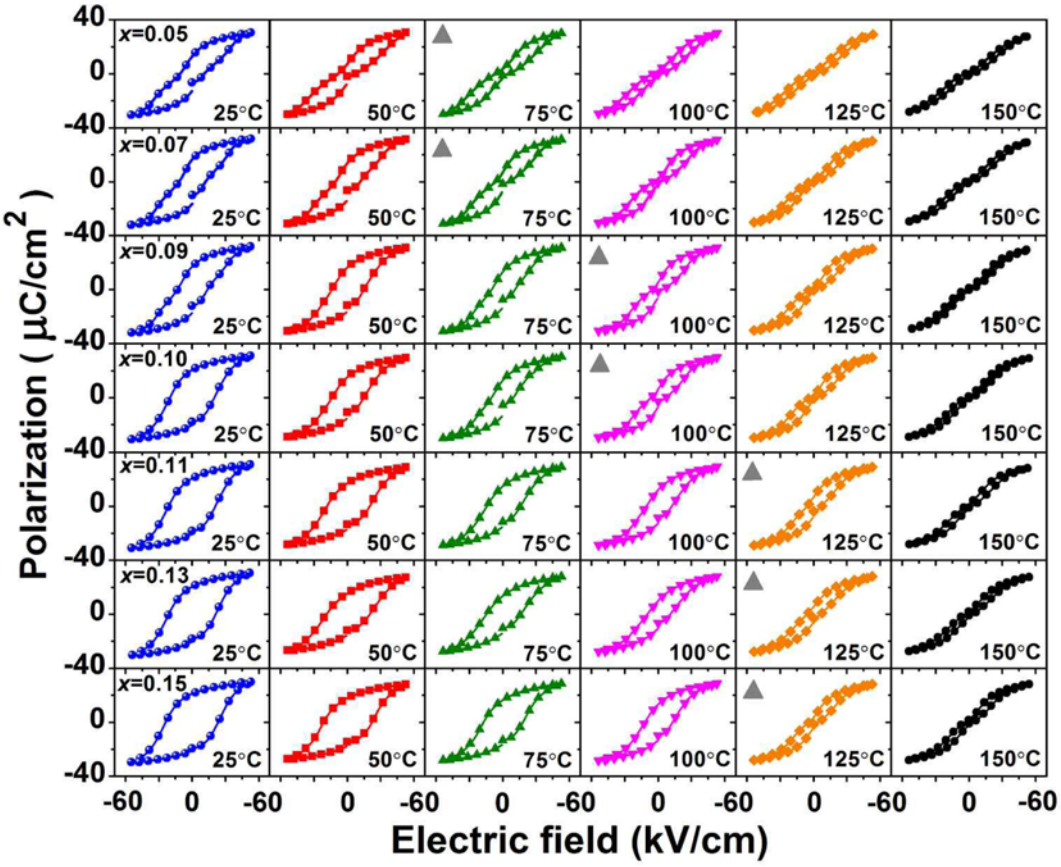

Fig. 8. Temperature dependent on polarization-electric field (*P*-*E*) hysteresis loops of (1-*x*)BNKT-*x*BTS ceramics, measured under an electric field of 55 kV/cm and a frequency of 1 Hz; where ▲ = indicates approximate onset temperature of the relaxor transition from a non-ergodic to ergodic state for each composition.

behavior was not evident even at 100°C. It clearly suggested that non-ergodic to ergodic relaxor transition was pushed to higher temperatures as the BTS content increased. It was consistent with Fig. 7, where depolarization temperature determined from temperature dependence of permittivity increased as the amount of BTS increased in the solid solution.

4. CONCLUSIONS

The (1-*x*)$Bi_{0.5}(Na_{0.80}K_{0.20})_{0.5}TiO_3$-*x*$Ba(Ti_{0.90}Sn_{0.10})O_3$ or (1-*x*)BNKT-*x*BTS (when x = 0.05 - 0.15 mol fraction) ceramics within the MPB region were successfully synthesized by a conventional mixed oxide method. In this MPB region, varying fraction of rhombohedral and tetragonal ferroelectric phases of this system was found throughout the whole composition range with tetragonal phase becoming dominant at higher BTS content. The sample near the region (*i.e.* x = 0.10 - 0.11) showed an improvement of electrical properties compared to that of other compositions. The relative amount of rhombohedral and tetragonal structure as well as lattice expansion caused the non-ergodic to ergodic transition temperature to be higher with increasing BTS content. In this study, it seemed that the optimum composition (x = 0.10 - 0.11) was obtained when nearly equal fraction of rhombohedral and tetragonal phases was present in the system at which the temperature of maximum permittivity (T_m = 333°C) and relatively good dielectric (ε_r = 1770, $tan\delta$ = 0.0746), ferroelectric (P_r =20.60 μC/cm^2) and piezoelectric properties (d_{33} = 227 pC/N, d^*_{33} = 445 pm/V and S_{max} = 0.24%) were obtained.

ACKNOWLEDGEMENTS

This work is financially supported by the Thailand Research Fund (TRF) (Grant no. RSA5780032). The Faculty of Science and the Graduate School, Chiang Mai University, Materials Science, School of Mechanical, Industrial and Manufacturing Engineering, Oregon State University, USA are also acknowledged. P. Jaita would like to acknowledge financial support from the TRF through the Royal Golden Jubilee Ph.D. Program.

REFERENCES

1. S. H. Lee, H. J. Kim, and Y. H. Lee, *Electron. Mater. Lett.* **8**, 289 (2012).
2. T. Takenaka, H. Nagata, Y. Hiruma, Y. Yoshii, and K. Matumoto, *J. Electroceram.* **19**, 259 (2007).
3. A. Sasaki, T. Chiba, Y. Mamiya, and E. Otsuki, *Jpn. J. Appl. Phys.* **38**, 5564 (1999).
4. K. Yoshii, Y. Hiruma, H. Nagata, and T. Takenaka, *Jpn. J. Appl. Phys.* **45**, 4493 (2006).
5. A. Ullah, C. W. Ahn, A. Hussain, I. W. Kim, H. I. Hwang, and N. K. Cho, *Solid State Commun*. **150**, 1145 (2010).
6. A. Ullah, C. W. Ahn, S. Y. Lee, J. S. Kim, and I. W. Kim, *Ceram. Int.* **38S**, S363 (2012).
7. Z. W. Chen and J. Q. Hu, *Adv. Appl. Ceram.* **107**, 222 (2008).
8. P. Jaita, A. Watcharapasorn, and S. Jiansirisomboon, *Electron. Mater. Lett.* **9**, 437 (2013).
9. P. Jaita, A. Watcharapasorn, D. P. Cann, and S. Jiansirisomboon, *J. Alloy Compd.* **596**, 98 (2014).
10. Y. R. Zhang, J. F. Li, and B. P. Zhang, *J. Am. Ceram. Soc.* **91**, 2716 (2008).
11. H. E. Swanson and R. K. Fuyat, *Natl. Bur. Stand. Circ. (U.S.) 539.* **3**, 44 (1954).
12. R. D. Shannon, *ActaCryst*. **A32**, 751 (1976).
13. Y. J. Dai, X. W. Zhang, and K. P. Chen, *Int. J. Appl. Ceram. Technol.* **8**, 423 (2011).
14. W. Zhao and R. Zuo, *Ceram. Int.* **39**, 9121 (2013).
15. W. C. Lee, C. Y. Huang, L. K. Tsao, and Y. C. Wu, *J. Alloy Compd.* **492**, 307 (2010).
16. G. A. Smolenskii, V. A. Isupov, A. I. Agranovskaya, and N. N. Krainik, *Sov. Phys. Solid State.* **2**, 2651 (1961).
17. D. Lin, K. W. Kwok, and H. L. W. Chan, *Solid State Ionics* **178**, 1930 (2008).
18. G. Fan, W. Lu, X. Wang, F. Liang, and J. Xiao, *J. Phys. D: Appl. Phys.* **41**, 035403 (2008).
19 S. T. Zhang, B. Yang, and W. Cao, *Acta Mater.* **60**, 469 (2012).
20. B. Wang, L. Luo, F. Ni, P. Du, W. Li, and H. Chen, *J. Alloy Compd.* **526**, 79 (2012).
21. A. Hussain, A. Zaman, Y. Iqbal, and M. H. Kim, *J. Alloy Compd.* **574**, 320 (2013).
22. W. Jo, R. Dittmer, M. Acosta, J. Zang, C. Groh, E. Sapper, K. Wang, and J. Rödel, *J. Electroceram.* **29**, 71 (2012).
23. J. Li, F. Wang, C. M. Leung, S. W. Or, Y. Tang, X. Chen, T. Wang, X. Qin, and W. Shi, *J. Mater. Sci.* **46**, 5702 (2011).
24. W. Jo, T. Granzow, E. Aulbach, J. Rodel, and D. Damjanovic, *J. Appl. Phys.* **105**, 094102 (2009).
25. X. Wang and B. Li, *Solid State Commun.* **149**, 537 (2009).
26. T. Takenaka, H. Nagata, and Y. Hiruma, *Jpn. J. Appl. Phys.* **47**, 3787 (2008).